Biomedicine & Pharmacotherapy 153 (2022) 113475

Contents lists available at ScienceDirect

Biomedicine & Pharmacotherapy

journal homepage: www.elsevier.com/locate/biopha

Fractions of *Hoslundia opposita* Vahl and hoslundin induced apoptosis in human cancer cells via mitochondrial-dependent reactive oxygen species (ROS) generation

Abosede Christiana Ajibare [a,*], Osaretin Albert Taiwo Ebuehi [a], Rahmat Adetutu Adisa [a], Margaret Oluwatoyin Sofidiya [d], Joseph A.O. Olugbuyiro [b], Kolajo Adedamola Akinyede [c], Helen Adeola Iyiola [a], Yusuf Adeyemi Adegoke [e], Sylvester Ifeanyi Omoruyi [c], Okobi Eko Ekpo [c]

[a] Department of Biochemistry, Faculty of Basic Medical Sciences, College of Medicine, University of Lagos, Lagos, Nigeria
[b] Department of Chemistry, Covenant University, PMB 1023 Ota, Ogun State, Nigeria
[c] Department of Medical Bioscience, Faculty of Natural Sciences, University of the Western Cape, Bellville, Cape Town 7530, South Africa
[d] Department of Pharmacognosy, Faculty of Pharmacy, College of Medicine, University of Lagos, Lagos, Nigeria
[e] School of Pharmacy, University of the Western Cape, Bellville, Cape Town 7530, South Africa

ARTICLE INFO

Keywords:
Hoslundia opposita Vahl
Cancer
Chemotherapy
Tumourigenic
Hoslundin
Natural products

ABSTRACT

Background: Cancer remains one of the leading causalities of several morbidity and mortality with negative impact on global economy due to low workforce and management/treatment cost. A number of conventional therapies have been explored in the management/treatment of cancer including chemotherapeutic intervention, radiotherapy, and surgery. Among these treatment modalities, chemotherapy remains the most popular first line of intervention in management/treatment of cancer, and natural products have been implicated as the main source of antineoplastic agents with phenomenal efficacy. However, current antineoplastic agents suffer from lack of selectivity and specificity necessitating the need for further research in the search for novel anticancer drug molecules.

Methods: In this present study, the anticancer activity of *Hoslundia opposita* leaves extracts were tested against a number of cell lines including human hepatoma cell line (HepG2), human breast cancer cell lines (MDA-MB-231), intestinal epithelial cell lines (Caco-2), and human keratinocyte HACAT cell lines. A bio-guided fractionation assay and the structural elucidation of the pure isolate (hoslundin) was conducted by 1D and ^{2}D NMR spectroscopy. The cell viability, colony formation, and apoptotic activities were investigated using MTT assay, clonogenic assay, and caspase − 3 and − 7 kits respectively. Flow cytometry was employed in assessing the altered cell cycle expression. The production of the intracellular reactive oxygen species (ROS) levels and the reduction of the mitochondrial membrane potential (MMP) was determined at the cellular level using fluorescent probe dyes dihydro-fluorescin diacetate (DCFH-DA) and tetramethylrhodamin (TMRE), respectively.

Results: The *H. opposita* fractions and its pure isolate (hoslundin) demonstrated a potent cytocidal activity against the tumorigenic cells (HepG2, MDA-MB-231, Caco-2) at concentration ranging from 25 to 100 μg/mL. The inhibition of the colony formation was significantly observed in HepG2 cell lines. More so, the cellular viability of the normal cells (HaCaT) was relatively unchanged in the presence of *H. opposita* fractions and its isolate proving the selectivity of the compounds towards tumourigenic cells. The *H. opposita* fractions and hoslundin exerted their anticancer activity via cell cycle arrest with the accumulation of the DNA content at the S-phase, activation

Abbreviations: HO1, Crude methanol extract; HO2, Hexane/Ethyl acetate 90:10 fraction; HO3, Hexane/Ethyl acetate 70:30 fraction; HO4, Hexane/Ethyl acetate 50:50 fraction; HO5, Hexane/Ethyl acetate 30:70 fraction; HO6, Ethyl acetate 100% fraction; HO7, Ethyl acetate:Methanol 50:50 fraction; CDKs, cyclin-dependent kinases; F-6, combined fractions; HepG2, human hepatoma cell line; MDA-MB-231, human breast cancer cell lines; Caco-2, Intestinal epithelial cell lines; HACAT, human keratinocyte cell lines; DCM, Dichloromethane; Hex, Hexane; EtOAc, ethyl acetate; MeOH, Methanol; TLC, Thin layer chromatography; NMR, Nuclear magnetic resonance; $CDCL_3$, Deuterated chloroform; HR-ESIMS, High resolution electron spray ionization mass spectrometry; DMEM, Dulbecco's modified eagles medium; G1/S, Gap1/ synthesis; G2/M, Gap 2/ Mitotic; DCFH-DA, Dihydro-fluorescin diacetate; TMRE, Tetramethylrhodamin; CCP, carbonyl cyanide m-chlorophenyl hydrazine; MMP, mitochondrial membrane potential; MTT, 4, 5- dimethylthiazol-2yl)-2, 5-diphenyl tetrazolium bromide; ROS, reactive oxygen species.

* Corresponding author.
E-mail address: boseajibare@gmail.com (A.C. Ajibare).

https://doi.org/10.1016/j.biopha.2022.113475
Received 7 June 2022; Received in revised form 21 July 2022; Accepted 23 July 2022
Available online 12 August 2022

of apoptosis in the caspase 3,7 activities and depolarized mitochondrial membrane potential mediated by mitochondrial-dependent ROS generation in the treated tumor cells.
Conclusion: The anticancer activities of *Hoslundia opposita* Vahl and hoslundin exhibited significant efficacy against tumor cells and well tolerated in the presence of normal cells making them a potential antineoplastic agent.

1. Introduction

Cancer remains one of the leading causalities of several morbidity and mortality with negative impact on global economy due to low work force and management/treatment cost [1,2]. According to International Agency for research on Cancer, an estimated 10 million cancer-related deaths was projected in 2020 [1]. Several conventional therapies have been explored in the management/treatment of cancer including chemotherapeutic intervention, radiotherapy, and surgery. Among these treatment modalities, chemotherapy remains the most popular first line of intervention in the treatment of cancer, and natural products have been implicated as the main source of antineoplastic agents with phenomenal efficacy [3,4]. The potential of natural plant products in cancer treatment and their aid in the attainment of therapeutic efficacy has gained considerable attention in recent years [5,6].

Compounds such as curcumin, etoposide, camptothecin, and paclitaxel are plant derived antineoplastic agents with efficacious anticancer dispositions including the disruption of tumourigenic cells growth by apoptosis and the inhibition of cancer cells proliferation [7,8].

Hoslundia opposita Vahl (*H. opposita*) is an herbaceous perennial shrub with characteristically round yellowish or orange berries which belong to the family of *Lamiaceae* with different local names in the different regions of Nigeria and have been utilized for the different treatment of various diseases including venereal diseases, herpes, and skin diseases [9–13].

The pharmacological activities of *H. opposita* have been extensively studied and reported [11,14–20]. Despite the several studies on its therapeutic actions in the treatment of several disease conditions, its mechanistic role as anticancer agent remains unexplored. This is typical of several plants derived compounds as their pharmacological actions are not fully explored [8].

Two major mechanisms are mostly explored in the anticancer activity of antineoplastic agents including apoptosis (i) and cell cycle arrest (ii). The apoptosis ensures DNA integrity while cell cycle modulates the cell growth. Moreover, the disruption of the cell cycle is known to foster tumor cells production and proliferation. Anticancer agents target the aberrant cell cycle thereby inducing tumor cell death by apoptogenicity. However, current antineoplastic agents suffer from lack of selectivity and specificity in distinguishing between healthy and abnormal cells leading to drug resistance, adverse drug reaction, alopecia, nausea, and aggravation of cancer pathogenesis. This has necessitated the need for further research in the search for ideal antineoplastic agents with high selectivity and specificity against tumor cells without causing damage to healthy cells [3,4]. This study will seek to investigate the molecular mechanisms of *Hoslundia opposita* Vahl fractions and its pure isolate (hoslundin) as anticancer agents against several mammalian cell lines including human hepatoma cell line (HepG2), human breast cancer cell lines (MDA-MB-231), intestinal epithelial cell lines (Caco-2), and human keratinocyte HACAT cell lines. A bio-guided fractionation and the structural elucidation of the pure isolates (hoslundin) was conducted by 1D and ^{2}D NMR spectroscopy. The cell viability, colony formation, and apoptotic activities were investigated using MTT, clonogenic and caspase 3/7 assays respectively. Flow cytometry was employed in assessing the altered cell cycle expression. The production of the intracellular reactive oxygen species (ROS) levels and the reduction of the mitochondrial membrane potential (MMP) was determined at the cellular level using fluorescent probe dyes dihydro-fluorescin diacetate (DCFH-DA**)** and tetramethylrhodamin (TMRE), respectively.

2. Materials and methods

2.1. Chemicals and tumourigenic cells

All chemicals and reagents used in this study were HPLC and analytical grade, procured from Sigma-Aldrich. *Hoslundia opposita* leaves was obtained from Nigeria. Mammalian cell lines including human hepatoma cell line (HepG2), human breast cancer cell lines (MDA-MB-231), intestinal epithelial cell lines (Caco-2), and human keratinocyte HACAT cell lines were supplied by the University of Western Cape, South Africa. The Dulbecco's modified eagle's medium (DMEM) with phenyl-red, Dulbecco phosphate-buffer saline (DPBS), the heat-inactivated fetal bovine serum (FBS, 10% (v/v)), the 100 μg/mL-penicillin: 100 unit/mL-streptomycin-amphotericin-B-mixture (PSA) and neutral red cell proliferation reagent (MTT) were purchased from Lonza® Group Ltd, Verviers, Belgium.

2.2. Plant collection and preparation

The leaves of *Hoslundia opposita* were obtained from the riverside in Agbara town, Ogun State (Nigeria) at a coordinate of 6°29'59.1"N 3°06'07.4"E. Plant material was identified and authenticated at the department of Botany, University of Lagos, Nigeria.

Hoslundia opposita leaves were rinsed, air-dried for 20 days at ambient temperature, and blended into a fine powder using a laboratory blender. The powdered *Hoslundia opposita* (2.329 kg) leaves was macerated in 5 L of 80% methanol in distilled water at ambient temperature for seven days. The extract was filtered using Whatman N0.1 filter paper and the solvent was evaporated by reduced pressure using rotary evaporator at 40 °C to obtain the methanolic crude extract of *H. opposita* (**HO1**, 116.4 g).

2.2.1. Fractionation of the crude extracts

Vacuum liquid chromatography (VLC) was performed with silica gel (0.063–0.2 mm mesh) as described by Olugbuyiro *et al.* [21]. Silica gel was loaded in hexane, and 80.74 g of the methanolic crude extract was dissolved in 4:1 Hexane/Ethyl acetate and mixed with 150 g of silica gel. The mixture was air-dried on filter paper at ambient temperature, and it was loaded into the VLC column. A gradient elution was employed for the mixture fractionation using solvent systems in order of increasing polarity including hexane/ethyl acetate (90:10, 3 L) **HO2**, (70:30, 8 L)

HO3, (50:50, 8.5 L) **HO4**, (30:70, 3 L) **HO5**; ethyl acetate (100%, 4 L) **HO6**; ethyl acetate/methanol, 50:50, 3 L) **HO7** and methanol (100%, 2.5 L) **HO8**. **HO2–7** represents the obtained fractions by various solvent or solvent systems. Fractions **HO2–4** were obtained using same solvent system (hexane/ethyl acetate) in increasing polarity ratio. The collected fractions were concentrated under reduced pressure by rotary evaporator, subsequently dried in a desiccator and stored in the freezer at − 4 °C. Cytotoxicity was conducted on the collected fractions. Fractions **HO5** and **HO6** were combined based on their cytotoxicity towards brine shrimp, human cancer cells and their thin-layer chromatography (TLC) profile.

2.2.2. Phytochemical screening

2.2.2.1. Qualitative and quantitative phytochemical screening. The preliminary phytochemical screening to test for alkaloids, flavonoids, saponins, tannins, phenols, steroids, cardiac glycosides and reducing sugar was performed on the methanolic crude extract of *H. opposita* leaves using the method described by Trease et al., Sofowora et al., Obadoni *et al.* [22,24,26].

The quantification of the secondary metabolites of the methanolic crude extract of *H. opposita* (**HO1**) leaves were achieved as described in the literatures [23–26]. Phenols were determined as described by the method of Waterhouse et al., [23]. Terpenoids, tannins, and steroids were determined as described by Sofowora et al., by the spectrophotometric method [24]. Flavonoids, alkaloids, and saponins were determined by methods described by [25,26].

2.2.2.2. Determination of antioxidant activity. The antioxidant activity of the extract were evaluated using 2,2-diphenyl-1-picrylhydrazyl (DPPH) radical scavenging activity [27], nitric oxide scavenging activity [28], and the reducing power [29], as previously described by Adisa *et al.* [30]. The total phenolic compounds, total flavonoids and total antioxidant capacity were determined by a modified Folin–Ciocalteu colorimetric method [9], aluminum chloride colorimetric method [31], and the pH differential spectrophotometric method [32], respectively.

2.2.3. Isolation of hoslundin

The purification of the combined extracts (**HO5** and **HO6**) was performed three times by column chromatography, scheme 1. The combined **HO5** and **HO6** (6.573 g) was subjected to column chromatography packed with silica gel and gradient elution using solvent system utilized in decreasing polarity. Hexane/ethyl acetate (90:10, [27] 0.8 L; 80:20, 0.8 L; 70:30, 1 L; 60:40, 1 L; 1:1, 1.2 L; 40:60, 1 L; 20:80, 1.2 L); hexane/ethyl acetate 1 L; followed by ethyl acetate/methanol (95:5, 0.6 L; 85:15, 0.8 L; 70:30, 0.8 L; 60:40, 0.6 L; 50:50, 0.5 L; 30:70, 0.4 L). Approximately 20 mL of eluents were collected into 566 vials and then pooled together based on their TLC profile to obtain 9 fractions (**F1 - F9**) which were concentrated under reduced pressure. Based on cytotoxicity and TLC profile, **fraction 6** (2.058 g) was selected and subjected to further purification using column chromatography packed with silica gel and solvent system of DCM/EtOAc (30:70, 0.2 L; 10:90, 2 L; 5:95, 0.6 L), followed by DCM 0.6 L, and then DCM/MeOH (98:2, 0.2 L; 95:5, 1.2 L; 90:10,0.8 L; 85:15, 0.4 L; 80:20, 0.6 L; 50:50, 0.6 L; 30:70, 0.4 L). This purification and isolation yielded 719 vials of 5mLs each, grouped based on their TLC profile to give 9 sub-fractions (**F6.1 – F6.9**). The third column chromatography was carried out on a Sephadex column using 100% methanol as eluent. Fractions were obtained and combined based

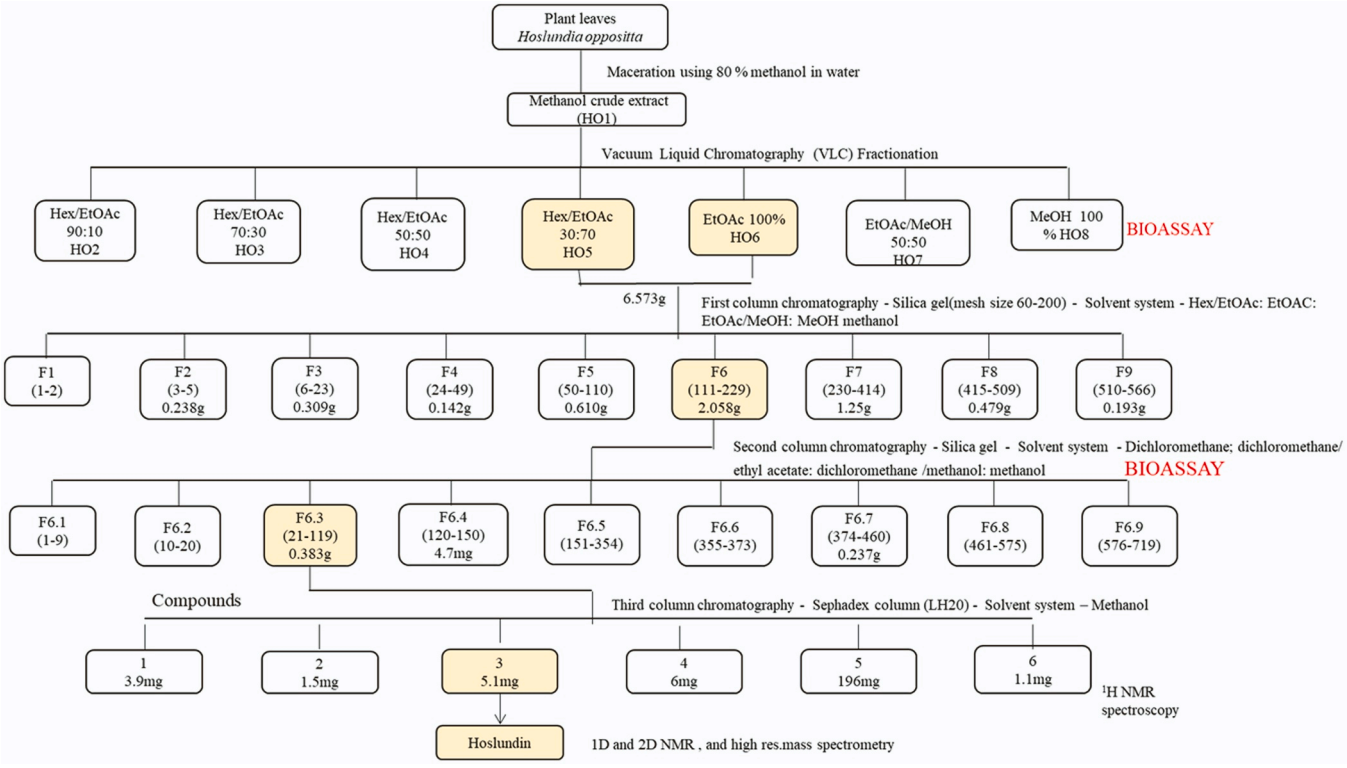

Scheme 1. Schematic diagram illustrating bio-assay guided fractionation of *Hoslundia opposita* leaves.

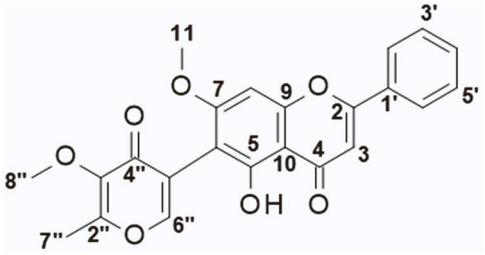

Fig. 1. Molecular structure of Hoslundin with numbering of carbon used for assignment of ^{13}C NMR spectra.

Table 1
Phytochemical screening of the methanolic crude extracts of *Hoslundia opposita* leaves.

Phytochemicals	Qualitative test	Quantitative test (mg/100 g)
Tannin	+	275.97 ± 0.28
Phenol	+	91.52 ± 0.09
Alkaloid	+	94.30 ± 0.41
Saponins	+	66.51 ± 0.15
Flavonoids	+	74.88 ± 0.83
Steroid	+	11.62 ± 0.24
Cardiac glycosides	+	21.63 ± 0.21
Reducing Sugar	+	20.74 ± 0.25

+ means present.

on TLC to give 6 fractions. The ^{1}H NMR profile of the 6 fractions confirmed fraction 3 to be pure and hence subjected to additional 1D and ^{2}D NMR analysis (Fig. 1).

2.2.4. Characterization of the isolated compound

The NMR spectra were recorded on a Bruker Avance 400 MHz spectrometer with deuterated chloroform ($CDCl_3$) as the solvent and referenced to the undeuterated solvent peaks ($CHCl_3\delta_H$ 7.26, δ_C 77.00) reported in parts per million (ppm). The high-resolution mass spectrometry data was obtained from a Waters Synapt G2-S mass spectrometer at the Central Analytical Facility of the University of Stellenbosch, South Africa. Sephadex LH-20® and silica gel 60 (0.063–0.2 mm mesh, Machery-Nagel) were used as the stationary phase in column chromatography. TLCs were performed on silica gel 60 F_{254} Aluminum sheets purchased from Merck KGaA, and visualization was achieved using UV light (254 nm and 365 nm) or iodine vapor.

The structural elucidation of the isolated compound was achieved by spectroscopic analysis using Nuclear Magnetic Resonance (1D and ^{2}D NMR) and High-resolution electrospray ionization mass spectrometry (HR-ESIMS). The obtained data are consistence with previous literature data. [17].

2.3. Cytotoxic activity

2.3.1. Cell lines and culture conditions

The human hepatoma cell line (HepG2), human breast cancer cell lines (MDA-MB-231), intestinal epithelial cell lines (Caco-2), and human keratinocyte HACAT cell lines were used in this study. The cell lines culturing and maintenance were conducted as described by Omoruyi *et al.* [36]. A gradient dose of 25–100 μg/mL of *H. opposita* and Hoslundin were prepared in supplemented media. IC_{50} [34] values for *H. opposita* and Hoslundin was obtained from the base study, and this was subsequently used as dose for the apoptotic assays, clonogenic, microscopic assays, cell cycle, reactive oxygen species (ROS), and mitochondrial membrane potentials (MMP) for 48 h.

2.3.2. Cell viability assay

The proliferation of the cells was determined using the colorimetric dye reduction assay [3-(4, 5-dimethylthiazol-2yl)− 2, 5-diphenyl tetrazolium bromide)] (MTT, Sigma-Aldrich). HepG2, MDA-MB-231, HACAT cell lines were seeded at a density of 5000 cells per well, while Caco-2 was seeded at 3000 cells per well in sterile 96 well plates and allowed to attach for 24 h. Followed by the administration of 100 μL (gradient dose) of *H. opposita* and Hoslundin against the cells whilst leaving the vehicular and static controls untreated with *H. opposita* and Hoslundin except for the addition of supplemented media or DMSO in supplemented media. The compound was allowed to incubate with cells for 48 h. After the treatment, the cells were washed with 100 μL of PBS and thereafter, fresh supplemented media was added and 10 μL of MTT solution (5 mg/mL) were added and allowed to incubate for 4 h. The media were carefully removed from each cell and 100 μL of DMSO to solubilize the purple formazan crystals added. Optical density (OD) was read at 570 nm using a microplate reader (BMG Labtech Omega® POLAR Star), and the mean cell proliferation was calculated relative to the control. The IC_{50} was calculated using Graphpad Prism 6 software (Graphpad®) from triplicate replicate measurements [33].

$$Percentage(\%)\ cell\ proliferation = \frac{Optical\ density\ of\ treated\ cells\ \times\ 100\%}{Optical\ density\ of\ control\ cells}$$

2.4. Caspase -3 and -7 activities

Caspase 3 and 7 activities were measured on the cancer cells using a Caspase-Glo 3/7® Assay kit (Promega, Madison, WI, USA). The experimental procedure of Caspase 3/7 activity is described as follows: The cells were plated at a concentration of 5000 cells/well in white-walled 96-well plates. Cells were treated with the fraction of their IC_{50} values and incubated for 48 h alongside the positive and negative controls. Caspase-Glo 3/7 reagents were added to the wells in a final volume of 200 μL and subsequently incubated at ambient temperature for 30 mins. Luminescence was measured at 520 nm using a microplate reader (BMG Labtech Omega® POLAR Star). The mean apoptotic activity was

Table 2
Antioxidant capacities of crude extracts and fractions of *Hoslundia opposita leaves*.

Plant Extracts	DPPH (μg/mL)	Reducing power (μg/mL)	Nitric Oxide (μg/mL)	TP (mg/100 g)	TAC (mg/100 g)	TF (mg/100 g)
HO1 (crude Extract)	**2.42** * **	**5.25** * **	**1.52**	35.95 ± 0.28[a]	50.90 ± 0.47[a]	45.46 ± 0.45a
HO2 (Hex/ EtOAc, 90:10)	2.00 * *	4.91 * **	4.82 * *	24.16 ± 0.17[b]	64.63 ± 0.46[b]	34.47 ± 0.19[b]
HO3 (Hex/ EtOAc, 70:30)	2.12 * *	4.35 * **	2.44 *	26.97 ± 0.61[c]	65.49 ± 0.40[c]	39.97 ± 0.26[c]
HO4 (Hex/ EtOAc, 50:50)	2.24 * *	4.75 * **	2.46 *	27.09 ± 1.88[d]	55.56 ± 0.35[d]	29.52 ± 0.13[d]
HO5(Hex/ EtOAc 30:70)	1.53 *	4.34 * *	1.46	46.22 ± 0.45[e]	72.39 ± 0.81[e]	43.46 ± 0.33[e]
HO6 (EtOAc, 100%)	1.74 *	4.19 *	1.86	39.19 ± 0.44 [f]	74.23 ± 0.29 [f]	45.23 ± 0.51 [f]
HO7 (EtOAc: MeOH, 50:50)	2.06 * *	5.17 * **	2.37 *	29.59 ± 0.33 [g]	41.63 ± 0.29 [g]	30.57 ± 0.06 [g]
Ascorbic acid	1.17	3.04	1.05			

Each value of the total phenols, total flavonoids, and total antioxidant capacity represent the mean± standard deviation of triplicate replicate values with *, ***, **, a, b,c,d,e,f,g are significantly different at $P < 0.05$ according to ANOVA/turkey's multiple-comparison tests. DPPH (1,1-diphenyl-2-picrylhydrazyl) radical scavenging activity; TP- Total Phenol; TAC- Total antioxidant capacity; TF-Total Flavonoids.

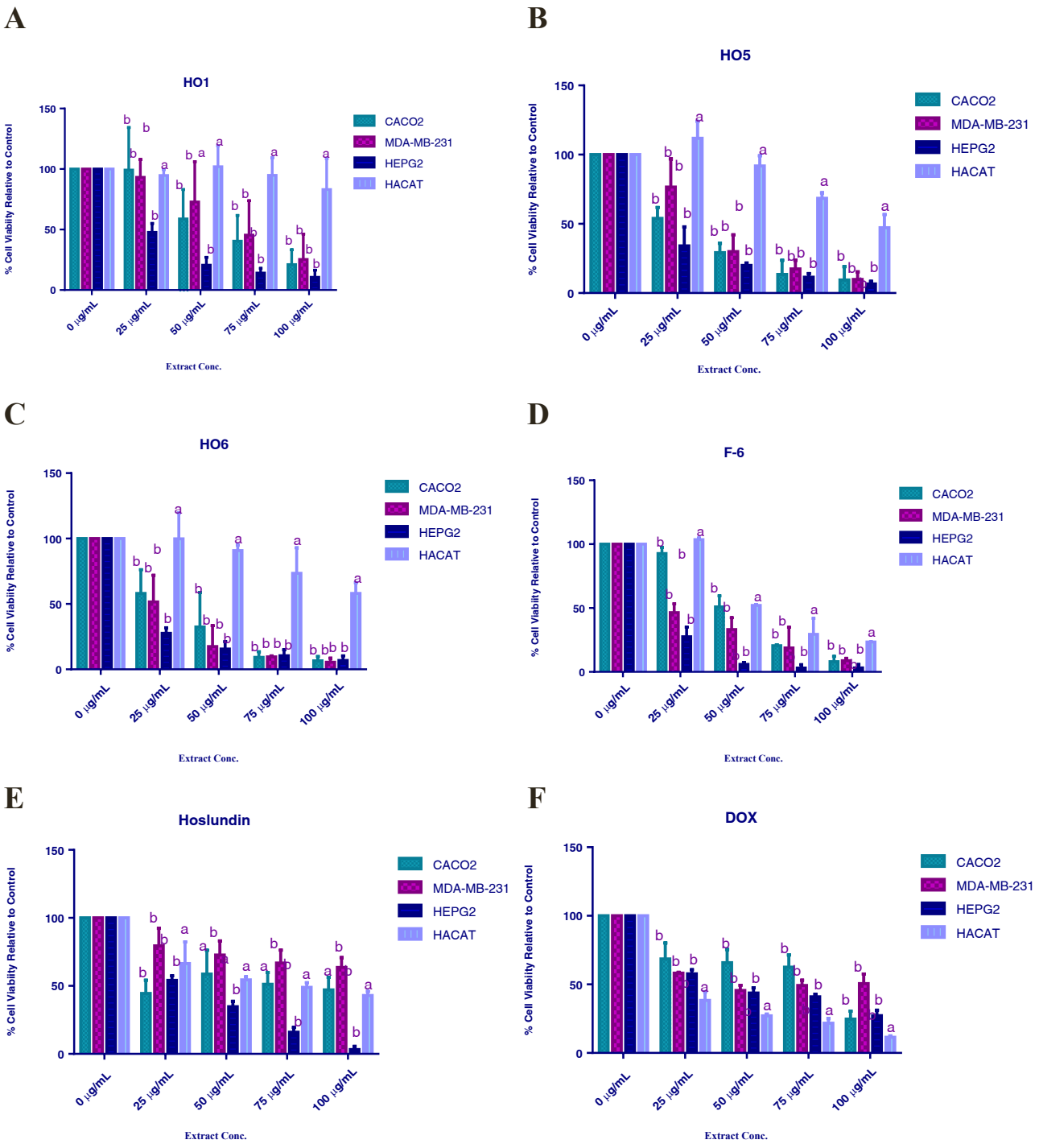

Fig. 2. Percentage cell viability of cancer (HepG2, Caco-2 and MDA-MB-231) and normal cells (HACAT) treated with selected fractions of *Hoslundia opposita* leaves and positive control drug doxorubicin (DOX) in increasing concentrations (0–100 µg/mL) for 48 h. A-E show a dose dependent decrease in cell viability of the cancer cells in relative to their control. Although, A-D show selective growth inhibition against cancer and normal cell line of HO1, HO5, HO6, and F-6 compared to the E and F (Hoslundin and DOX). Results show bars with the mean percentage cell viability ± SEM relative to the control of data obtained from triplicate replicate measurements.

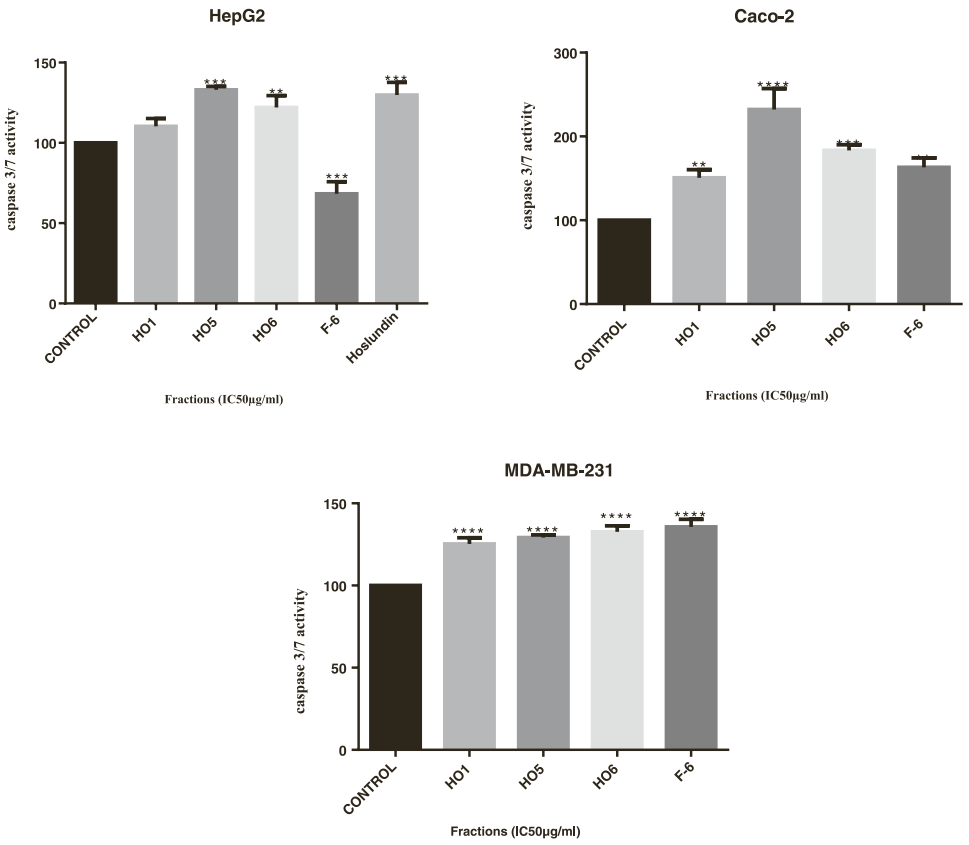

Fig. 3. The apoptotic activity of the fractions after 48hrs treatment on HepG2, Caco-2 and MDA-MB-231 cell lines. Data are expressed as mean ± SEM of three repeats of experiment. Values with **, ***, **** are significantly different ($P \leq 0.05$) according to ANOVA and Tukey's multiple comparison tests.

calculated relative to control using Graphpad Prism 6 software (Graph pad Software, San Diego, CA, USA) from two experimental repeats.

2.5. Clonogenic assay

Cancer cells were plated in 6 cm dishes according to their densities and left for 24 h to attach. They were treated using the IC_{50} (Table 4) of the fractions of the plants for 48 h. Cells were trypsinised, re-suspended in 2 mL of culture media, counted, and re-seeded at 500 cells per dish (35 mm). The cells were incubated and monitored using the untreated cells for ten days and stained. Cells were washed in PBS, fixed with methanol and glacial acetic acid solution (3:1), fixed cells were stained with 0.5% crystal violet in methanol, and a final wash with PBS and distilled water was done to get a clear image of the dishes. Images of the dishes were taken, and areas covered by colonies were calculated using Image J software [35] and expressed as a percentage of control set to a hundred percent.

2.6. Microscopy assay

To establish the morphological changes related with the treatments on HepG2, Caco-2 and MDA-MB-231 cell lines. The cell lines were plated on 60 mm dishes and left for 24 h to settle. Growth media was changed and cells were treated with the IC_{50} *H. opposita* and hoslundin (Table 4) for 48 h, and changes in their morphology were monitored using an inverted light (Olympus, USA) and photographs were taken with Zeiss Axiocam (Germany) camera [36].

2.7. Cell cycle assay

The cells were seeded at their various densities as described above for 24 h and treated with the IC_{50} (Table 4) of the fractions and hoslundin for 48 h on each cell lines. After treatment, media from each well-containing cells were transferred to 15 mL conical tubes. Cells were washed with 1 mL PBS and transferred into the corresponding 15 mL conical tubes containing the floating cells. Cells were trypsinised, incubated at 37 °C for 1 mins, and washed twice with PBS (transferred into the 15-mL conical tubes) centrifuged at 3000 rpm for 5 mins. Supernatants were discarded, pellets were re-suspended in 2 mL of cold PBS and fixed in 8 mL of ice-cold 70% ethanol. DNA content of samples was determined by flow cytometry. Following fixation, samples were centrifuged at 3000 rpm for 5 mins, the supernatant was removed, and pellets were re-suspended in 500 µL of PBS. Samples were again centrifuged at 3000 rpm for 5 min, the supernatant was removed, the pellets were re-suspended in 300 µL of FxCycle™ PI/RNase (Molecular Probes, Life Technologies, UK) for 30 mins. Cell cycle analysis was done using the FACS Calibur flow cytometer (Beckman Coulter, USA), and data were analyzed using the Cell Quest Pro version 5.2.1. [36].

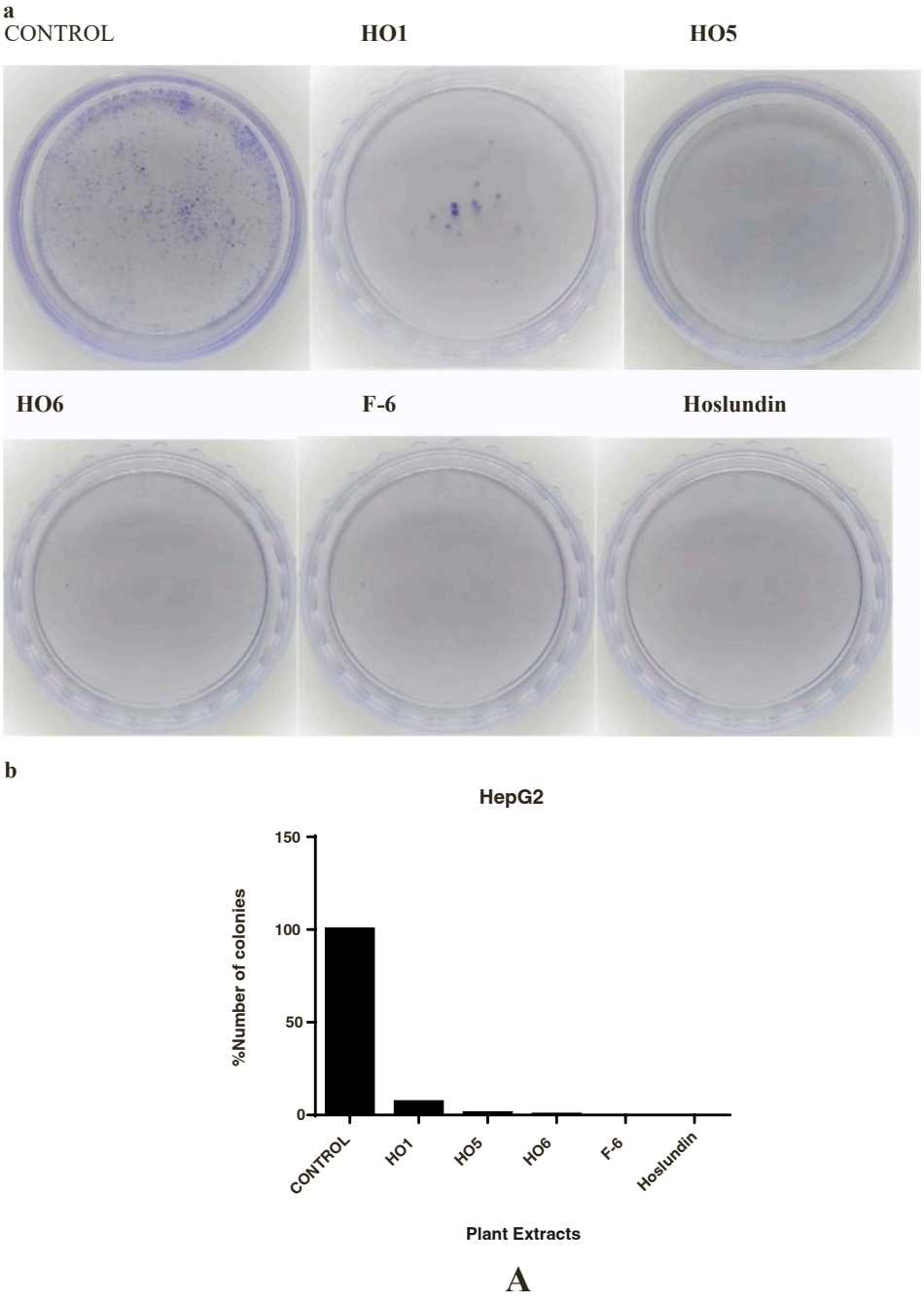

Fig. 4. (A)**:** Clonogenic view (a) of the fractions of *Hoslundia opposita* leaves and hoslundin. Bar charts (b) of clonogenic analysis on Hep G2 cell lines colony formation. Images of the dishes were taken, and areas covered by colonies were calculated using Image J software. Values with *, ** are significantly different ($P \leq 0.05$) according to ANOVA and Tukey's multiple comparison tests. (B): Clonogenic view (a) of the fractions of *Hoslundia opposita* leaves. Bar charts of clonogenic analysis on Caco-2 cell lines colony formation (b). Images of the dishes were taken, and areas covered by colonies were calculated using Image J software. Values with ***, **** are significantly different ($P \leq 0.05$) according to ANOVA and Tukey's multiple comparison tests. (C): Clonogenic view (a) of the fractions of *Hoslundia opposita* leaves. Bar charts of clonogenic analysis on MDA-MB-231 cell lines colony formation (b). Images of the dishes were taken, and areas covered by colonies were calculated using Image J software. Values with ***,**** are significantly different ($P \leq 0.05$) according to ANOVA and Tukey's multiple comparison tests.

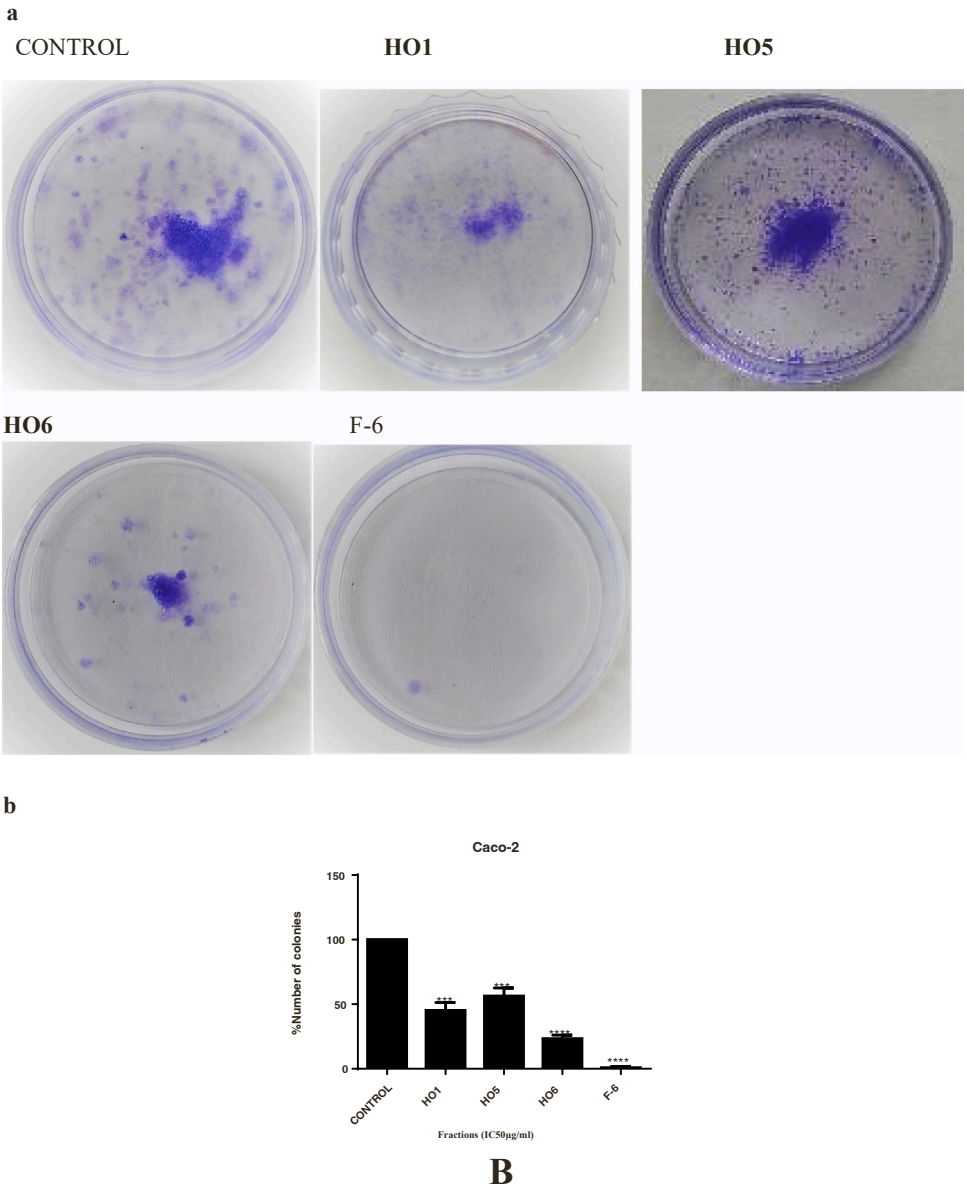

Fig. 4. (*continued*).

2.8. Assessment of intracellular reactive oxygen species ROS

Levels of intracellular ROS were determined using the fluorescent probe Dihydro-fluorescin diacetate (DCFH-DA) with some modifications [37]. Briefly, cell lines (5000 cells/well) were seeded into 96 well plates and treated after 24 h with *H. opposita* and hoslundin for 48 h. Control cells were incubated with 250 mM H_20_2, as a positive control for 15 mins. ROS activity in cells was determined by staining the cells with 20 μM DCFH-DA in dark at 37 °C for 60 mins, washed once with PBS, and 100 μL of PBS was added to each well, and fluorescence intensity of DCFH-DA was measured using a POLAR Star Omega BMG.

2.9. Measurement of mitochondrial membrane potential (MMP)

Mitochondrial membrane potential (MMP) was determined using the fluorescent dye, Tetramethylrhodamin (TMRE) according to the methods by Zamzami *et al.* [38]. Cells were seeded at 2000 per well in 96-well plates, incubated for 24 h, and treated with *H. opposita* and hoslundin for 48 h. Cells were treated with carbonyl cyanide m-chlorophenyl hydrazine (CCP) as positive control for 10 mins, supernatant was removed and washed with 100 μL PBS. Cell pellets were re-suspended in 100 μL PBS, and fluorescent intensity was measured at 544 nm using a microplate reader (BMG Labtech Omega® POLAR Star). The percentage mean was calculated relative to the control using

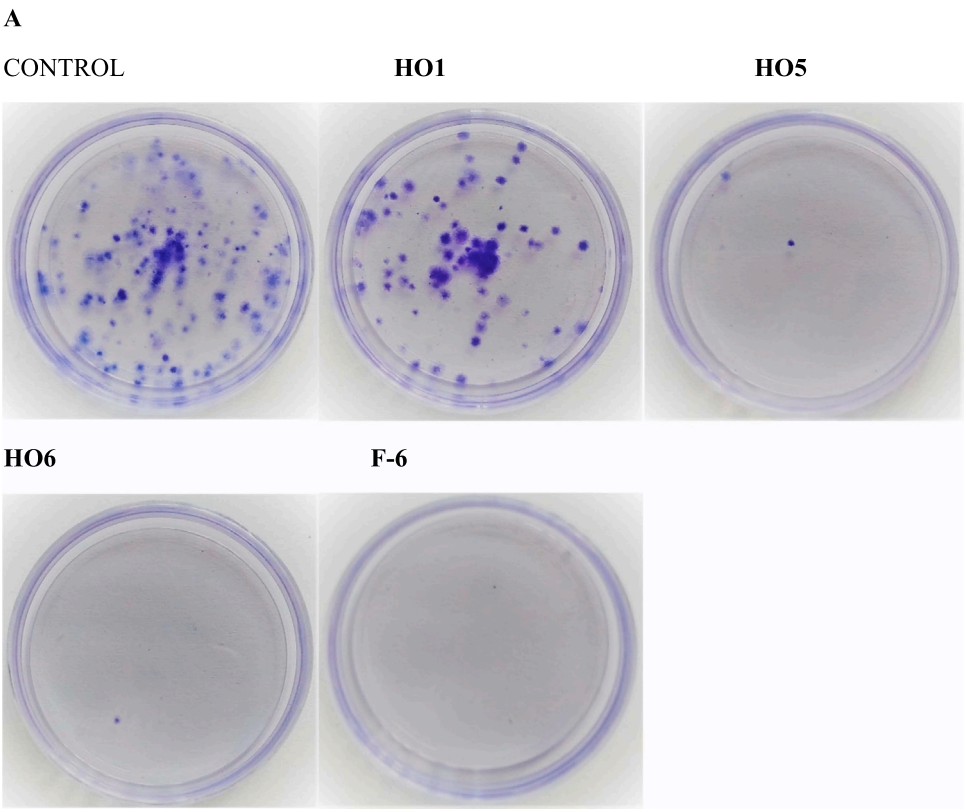

Fig. 4. (*continued*).

Graphpad Prism 6 software (Graphpad®) in triplicate replicate.

2.10. Statistical analysis

The data generated in this study were statistically analyzed using GraphPad Prism version 6 software and expressed as mean ± standard error of means (SEM) of the triplicate replicate measurements. The one-way analysis of variance (ANOVA) entails the investigation of the significance of difference between the treated (intra) and control groups and values were considered to be statistically significant at $P < 0.05$.

3. Results

The results of phytochemical screening and anticancer activities of *Hoslundia opposita* (HO) leaves are presented in this section. Phytochemical screening of the methanolic crude extract of *H. opposita* leaves (Table 1) demonstrated relatively high quantities of secondary metabolites which could be attributed to the choice of solvent(s) employed for the compound extraction. The order of increasing quantitative estimation of extracts are Tannins > alkaloids > phenols and flavonoids ranging between 275.97 ± 0.28 mg/mL and 74.88 ± 0.83 mg/mL.

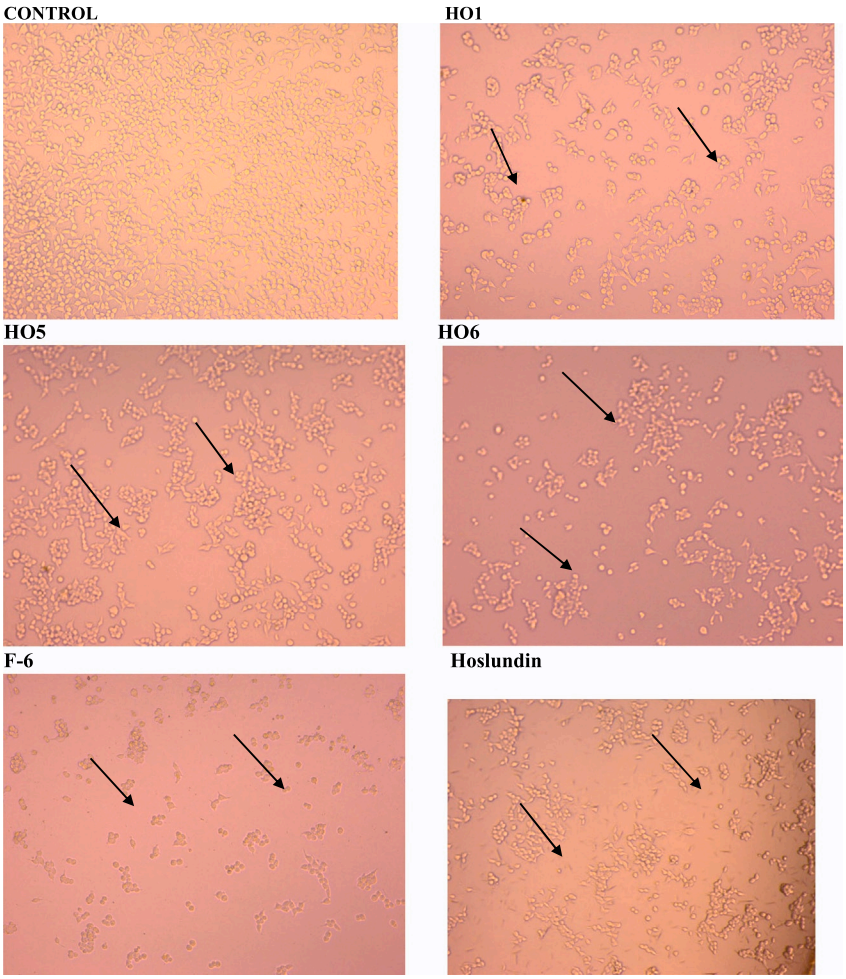

Fig. 5. (A): Photomicrographs of HepG2 cells treated with crude extract (23.18 μg/mL), Fractions HO4 (15 μg/mL), HO5 (11 μg/mL), F-6 (17 μg/mL) and Hoslundin (27 μg/mL) compared to the control cells (untreated cells). Cells were photographed using a microscope Zeiss Axiocam (Germany) camera. Arrows in treated cells indicates dissociation of cells, changes in their morphology and growth inhibition. (B): Microscopic images of Caco-2 cells treated with HO1 (62 μg/mL), HO4 (28 μg/mL), HO5 (30 μg/mL) and F-6 (51 μg/mL) compared with control. Caco-2 cell lines after 48 h treatment. Arrows indicates that the treated cells showed alterations in their morphology and reduction in growth as compared to the control cells (untreated cells). Characteristics of apoptotic events such as membrane blebbing, dark spots, a roundish cell that were not visible in the control group. Photomicrographs of the MDA-MB-231 cells treated with **HO1** (70 μg/mL), **HO4** (33μg/mL), **HO5** (26 μg/mL) and **F-6** (24 μg/mL) compared to control cells (untreated cells). Cells were photographed using a microscope Zeiss Axiocam (Germany) camera. The arrows indicate apoptotic events such as black spots, dissociation of cells and reduce growth

However, quantitative estimation of steroid, cardiac glycosides and reducing sugar were within an average of 17.33 ± 0.23.

The activities of the antioxidant capacities were evaluated using the IC_{50} of the antioxidant capacities which corresponds to the anticancer fractions that are able to scavenge 50% of the free radicals in the reaction mixture of the plants. Since low IC_{50} indicates a strong antioxidant capacity, fractions **HO5** (1.53 μg/mL) and **HO6** (1.74 μg/mL) showed a strong DPPH scavenging activity compared to other fractions in relative to their positive control ascorbic acid (1.17 μg/mL). This study also showed a trend that fractions **HO5** and **HO6** compared to other fractions of the plant have the best scavenging activities.

3.1. Identification and spectroscopic analysis of the purified Hoslundin

Hoslundin was identified as a white amorphous solid. The pure isolate (Hoslundin) showed HR-ESIMS *m/z* of 407.1130 [M + H] which is consistent to the calculated value 407.1131 corresponding to a molecular formula of $C_{23}H_{18}O_7$. The ^{1}H NMR spectrum displayed a characteristic de-shielded hydroxyl proton signal at δ_H 13.02 (s, 1 H, OH-5) followed by the aromatic signals resonating at 7.91 (dd, J = 7.9, 1.7 Hz, 2 H-2′6′), 7.73 (s, 1 H, H-6″), 7.55 (m, 3 H, H-4′, 2 H-3′5′), 6.70 (s, 1 H, H-3), 6.59 (s, 1 H, H-8), as well as two methoxy singlets at 3.91 (s, 3 H, OCH_3-8″), and 3.88 (s, 3 H, OCH_3-11), and a methyl singlet at 2.38 (s, 3 H, CH_3-7″). The ^{13}C NMR spectrum (Fig. 1) exhibited 21 carbon

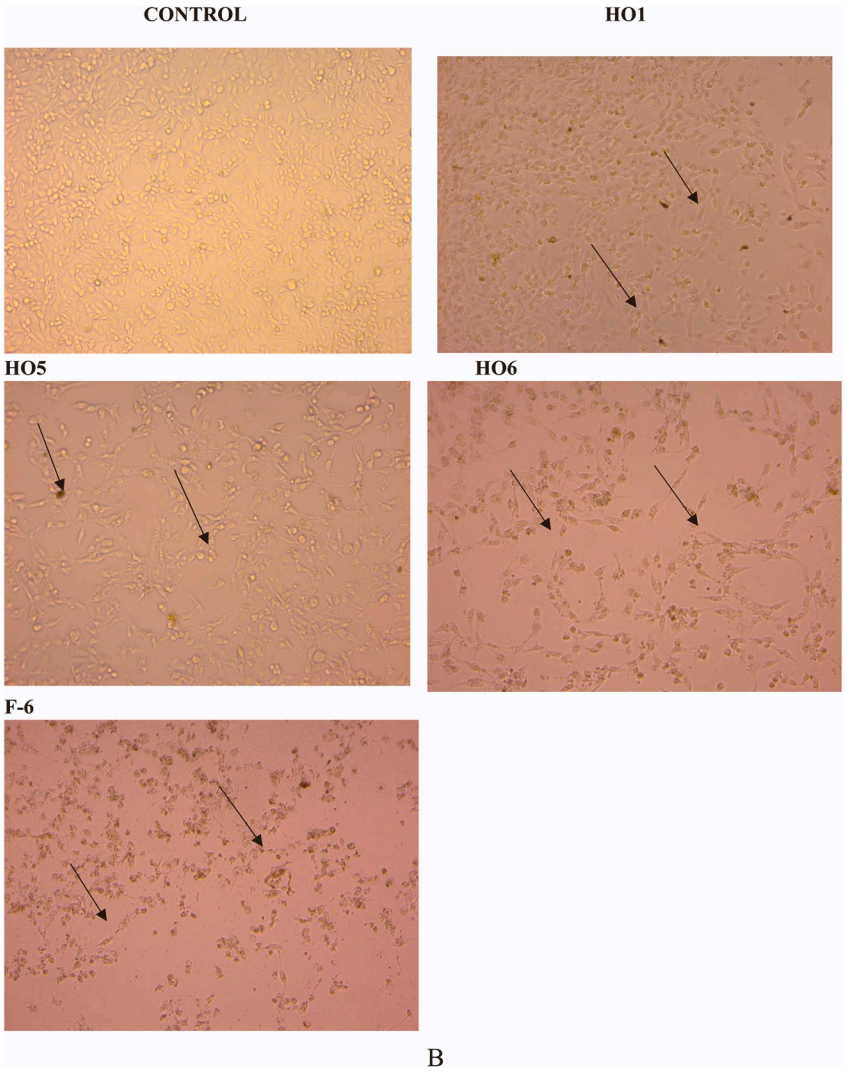

Fig. 5. (*continued*).

resonances, the ketone functionalities at positions 4 and 4″ resonated at δ_C 182.4 and 173.3, respectively. It also displayed the same chemical environment for C-3′, 5′ at δ_C 129.1 and C-2′,6′at δ_C 126.3 with higher peak intensities. The methoxy carbon resonances were observed at δ_C 60.1 (C-8″), and 56.4 (C-11), and up-field is the sp3 hybridized methyl carbon that resonated at δ_C 14.8 (C-7"), Table 2. The ^{2}D NMR data (HSQC, HMBC, and COSY) confirmed all the ^{1}H–^{13}C and ^{1}H–^{1}H correlations, affirming the assignments.

Preliminary bioassay using brine shrimp and cancer cell lines was employed in selection of the fractions used for further biological activity (data not included). **HO1**, **HO5**, **HO6**, **F-6** and positive control drug (Doxorubucin) and these fractions were chosen based on their phenomenal activity informing their evaluation on Caco-2, HepG2 and MDA-MB-231 using a dose dependent study (Fig. 2A-F) to establish IC_{50} dose which was subsequently used for other biological assay including caspase − 3 and − 7 activities, clonogenicity, microscopy evaluation, cell cycle assay, intracellular ROS quantification, mitochondrial membrane potential (MMP) test. IC_{50} represent the minimum inhibitory concentration of the compound in inhibiting at least half of the tumourigenic cells. All the fractions considered showed significant activity against the tumors except for relative innocuous activity against the normal cells (HaCaT) cell line. The compound activity was compared with doxorubicin, and it was found to afford better efficacy using the current cell lines, Fig. 2A-F.

The IC_{50} data of the compounds are presented in Table 4. The IC_{50} data of the fractions were found to outperform the doxorubicin with better efficacy and selectivity. Interestingly, the biochemical effector pathway of **HO1**, **HO5**, **HO6**, **F-6** and hoslundin induced apoptosis, were measured using caspase 3/7 caspase Glo kit (Promega), Fig. 3. Fractions **HO1**, **HO5**, **HO6**, and **F-6** show significant activation of caspases 3/7 in cancer cell lines. However, a significant decrease was observed in **F-6** treated cells of HepG2, while the hoslundin showed a significant increase in HepG2. Hence, these results imply apoptotic induction via the caspase cascade pathway.

The ability of cells to form colonies and survive treatment with the tested fractions were carried out using crystal violet dye staining, Fig. 4A–C. The colonies population of HepG2 and MDA-MB-231 compared to the Caco-2 cell lines were significantly reduced in the presence of *H. opposita* fractions, Fig. 4A–C. Specifically, the results presented in Fig. 4A–C demonstrated the possibility of fraction of HO to be irreparable including ability to slow down and prolong the growth of colonies formation. However, the most effective cell growth inhibition was observed on the HepG2 cell lines as shown in Fig. 4A.

Typical apoptosis changes were also investigated as shown in Fig. 5A–C in cancer cells lines after 48 h treatment with the *Hoslundia opposita* leaves fractions. The *H. opposita* leaves caused changes in the

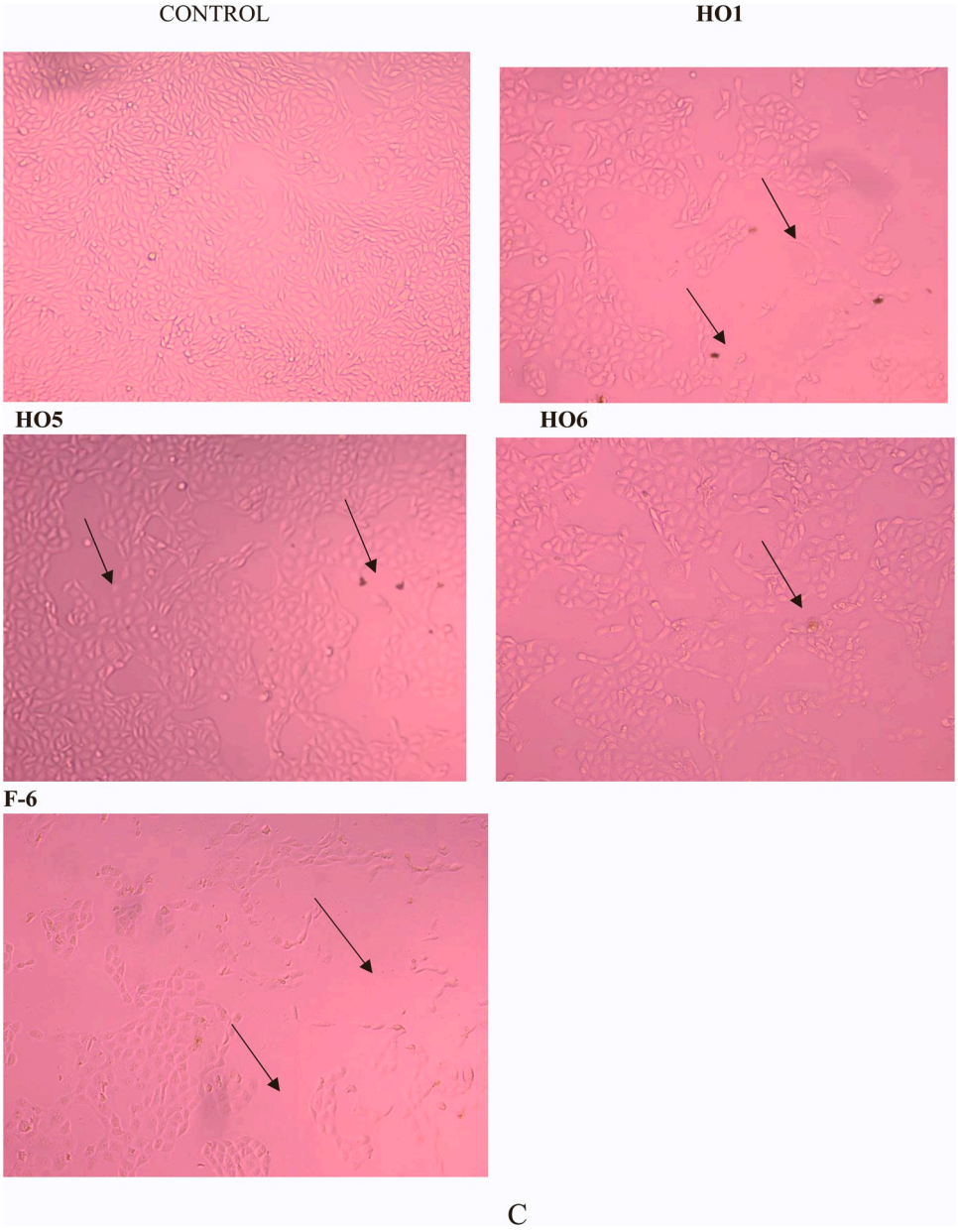

Fig. 5. (*continued*).

morphologies of the employed cell lines as indicated by the morphological parameters (roundish, dark spot and inhibition of growth) as observed in Fig. 5A–C. More so, the changes in growth inhibition by the fractions of *Hoslundia oppoita* can be attributed to the induction of apoptotic cell death in the cancer cell lines under study.

To understand the mechanism of the fractions of **HO** leaves mediated cell growth inhibition, cell cycle distribution was determined in cancer cells in Fig. 6A–C. The DNA content in HepG2 cells were arrested after treatment with the *H. opposita* fractions and Hoslundin. Moreover, *H. opposita* leaves fractions and Hoslundin induced a decrease in the percentage of cells in the G1/G0 phase and increase in the S-phase. The fractions did not show the arrest of MDA-MB-231 cell lines as compared to the control.

To determine whether the observed cell death was due to ROS-induced activity and disruption of MMP, treated cells were stained with florescent dyes for 48 h, Fig. 7. Fractions **HO5** and **HO6** of *H. opposita* leaves significantly increased ROS activity and caused a reduction in the MMP activity in HepG2, Caco-2 and MDA-MB-231 cells. Although, hoslundin caused a significant reduction in ROS and increased MMP activity in HepG2 cell lines.

4. Discussion

Natural anticancer compounds from plants are well recognized to be involved in mechanism-oriented targets that disrupt or mitigate other mechanisms that promote cancer cell proliferation and invasiveness [39,40]. Plant phytochemicals are adjudged to be effective anticancer agents in different cancer types from research findings. For example, flavonoids that belong to the polyphenols class exhibit effective inhibition of angiogenesis, proliferation, and metastasis through activation of apoptosis, important mechanisms of cancer therapy [41,42]. Plant chemicals act as antioxidant, maintaining redox status in cells by inhibiting oxidative stress, especially in pathological conditions such as cancer. Some of the antioxidants at higher concentrations act otherwise and induce reactive oxygen species in cells, a characteristic pro-oxidant property to promote cell death of cancer [43,44].

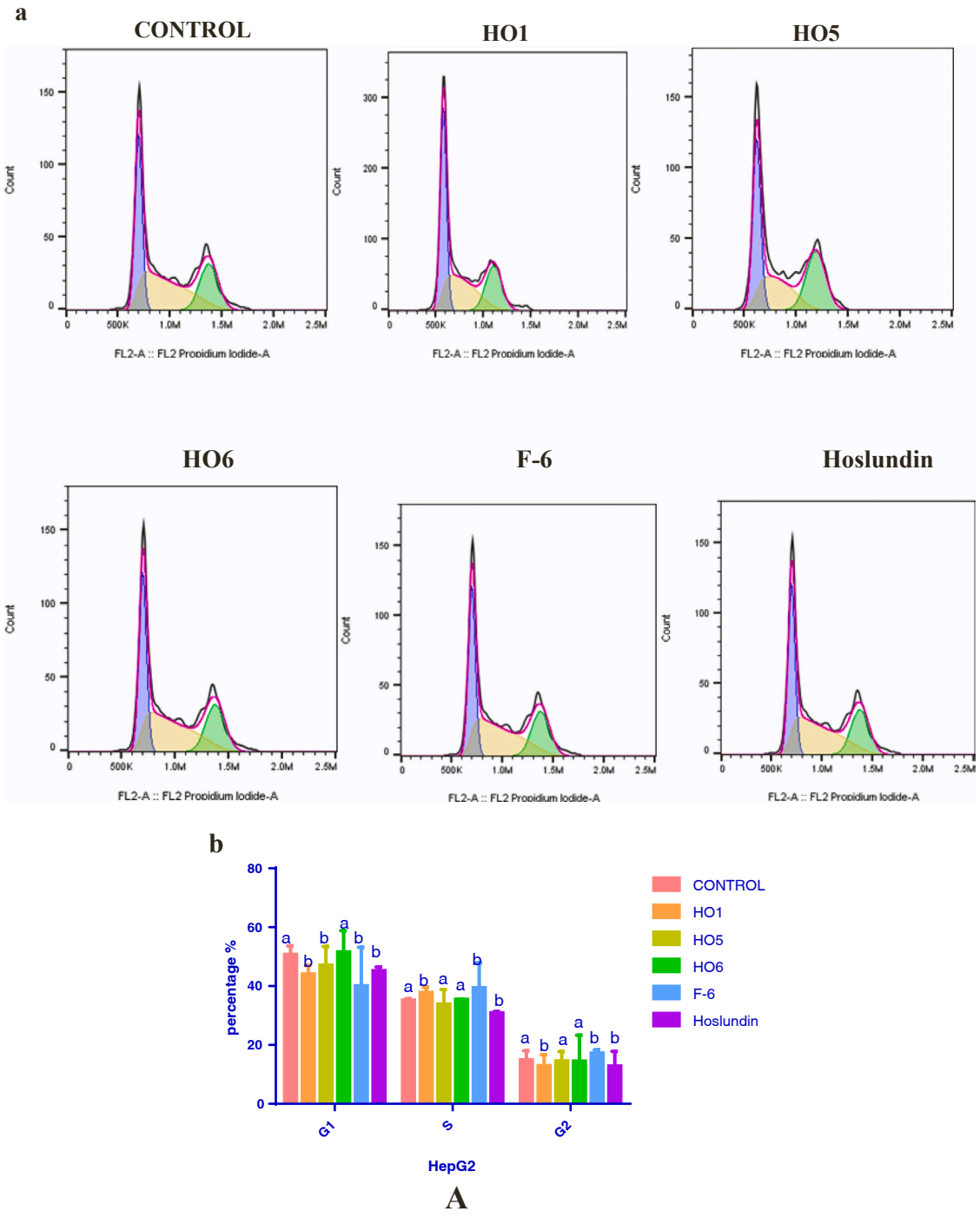

Fig. 6. (A): (a) Representative flow cytometry profile of HepG2 cells exposed to 48 h treatment and stained with propidium iodide for 30 mins. Different phases of the cycle are represented by blue (G1 phase), orange (S phase), green (G2 phase) and plots are representation of two individual experiments. (b) Bar graphs of HepG2 cells in the different phases of the cell cycle. Each bar represents the mean ± SEM of two repeated experiments, and their level of significance was measured at $P < 0.05$ between the control and the treated cells. The number of cells was expressed as the percentage of the total number of cells analyzed. (B): (a) Representative flow cytometry profile of Caco-2 cells exposed to 48 h treatment and stained with propidium iodide for 30 mins. Different phases of the cycle are represented by blue (G1 phase), orange (S phase), green (G2 phase) and plots are representation of two individual experiments (b) Bar graphs of Caco-2 cells in the different phases of the cell cycle. Each bar represents the mean ± SEM of two repeated experiments, and their level of significance was measured at $P < 0.05$ between the control and the treated cells. The number of cells was expressed as the percentage of the total number of cells analyzed. (C): (a) Representative flow cytometry profile of MDA-MB-231 cells exposed to 48 h treatment and stained with propidium iodide for 30 mins. Different phases of the cycle are represented by blue (G1 phase), orange (S phase), green (G2 phase) and plots are representation of two individual experiments (b) Bar graphs of MDA-MB-231 cells in different phases of the cell cycle. Each bar represents the mean ± SEM of two repeated experiments, and their level of significance was measured at $P < 0.05$ between the control and treated cells. The number of cells was expressed as the percentage of the total number of cells analyzed.

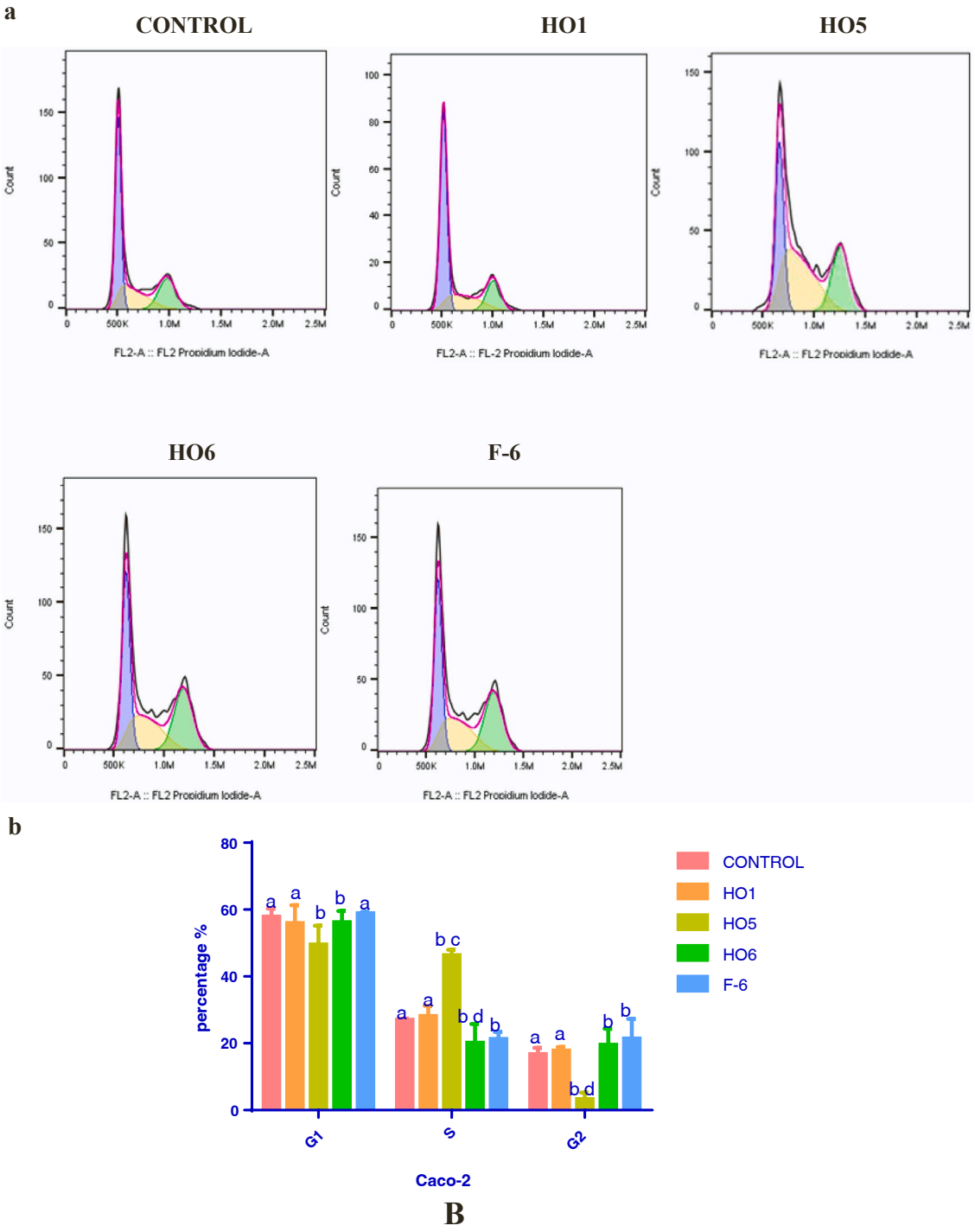

Fig. 6. (*continued*).

The bio-guided assay employed in this current study is to ensure that undesirable or antagonist of biological responses are excluded, thus improving bioavailability and pharmacokinetic profiles leading to better anticancer agent activity [45,46]. Hoslundin was previously isolated from *Hoslundia opposita* along with other pyrone-substituted flavonoids, and the spectroscopic data presented in Table 3 agrees with the literature reports [17].

The selectivity strategy achieved in this work revealed that Fractions **HO1**, **HO5**, **HO6**, **F-6** and Hoslundin showed a significant dose-dependent decrease in cell viability in cancer cell lines, which usually signifies a high cytotoxic effect, Fig. 2, and Table 4. At the same time, it is less toxic in a normal cell line which is in line with other anticancer-related studies [7,47–49]. This study shows that fractions **HO1**, **HO5**, **HO6**, **F-6**, and the purified bioactive compound, hoslundin showed a relative safety profile compared with standard drug doxorubicin on HACAT, a normal cell line (Fig. 2, and Table 4).

Findings of this study in Fig. 6A–C also indicates that Fractions **HO1**, **HO5**, **HO6**, and **F-6** accumulate in the S phase of the cell cycle, which implies the disruption of DNA synthesis and the G1 phase inhibits the progression of damaged DNA in HepG2 and MDA-MB-231 cell lines. In

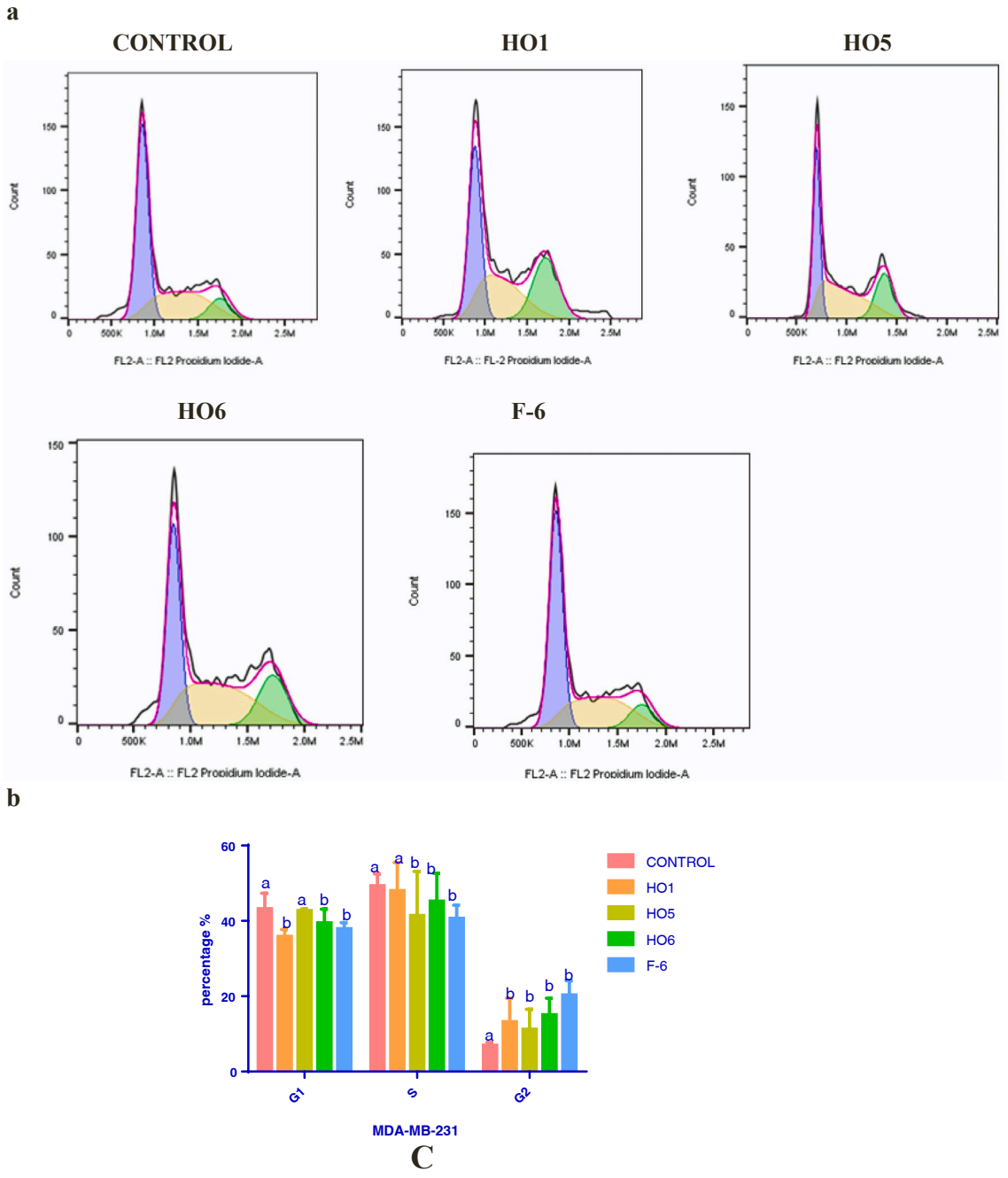

Fig. 6. (*continued*).

addition, all the fractions caused cell cycle arrest at the G1 phase as shown in Fig. 6A–C. However, it was noted that only fraction **HO1** induced cell cycle arrest in the S phase in the Caco-2 cell line, indicating that the cell cycle could be anticancer agent-specific. The arrest at various stages in the cell cycle that induces apoptosis has been explored as an essential strategy of natural products of crude and purified compounds as anticancer agents [51] where they promote cancer cell death. The study depicts that the apoptosis-inducing potential of the fractions **HO1**, **HO5**, **HO6**, **F-6** are attributed to an array of phytochemicals as shown in Table 1. The previous studies indicated that phenolic acid and some specific phytochemicals from natural products have an apoptotic effect on different cancers [50,52].

The apoptotic activity in Fig. 3 is indicative of the activation of caspases – 3 and 7, catalytic proteases from the treatment of **HO1**, **HO5**, **HO6**, **F-6**, and hoslundin in different cancer cell lines. The apoptotic events were significant and could be mediated intrinsically via mitochondrial transduction pathway. Furthermore, the results in Fig. 5A–C revealed the characteristics morphology of apoptosis showed patterns of cell death with respect to cell shrinkage, chromatin condensation, cell organelle degradation, and protein cleavage during **HO1**, **HO5**, **HO6**, **F-6**, and hoslundin treatment in the cell lines. The exhibited characteristics of apoptosis could be attributed to pattern of cell death [7,53].

The reactive oxygen species (ROS) mediated apoptotic death denotes manipulations of ROS level by targeting the redox system, Fig. 7. This vital strategy of anticancer agent selectively kills cancer cells thus allows for the survival of the normal cells [54]. For instance, some ROS inducers that target ROS generating system have been implicated in causing toxicity with reported non-bioavailability. As a result, ROS inductors failing therapeutic intention in cancer cells in clinical settings. The mechanism of ROS in causing the death of cancer cells involved

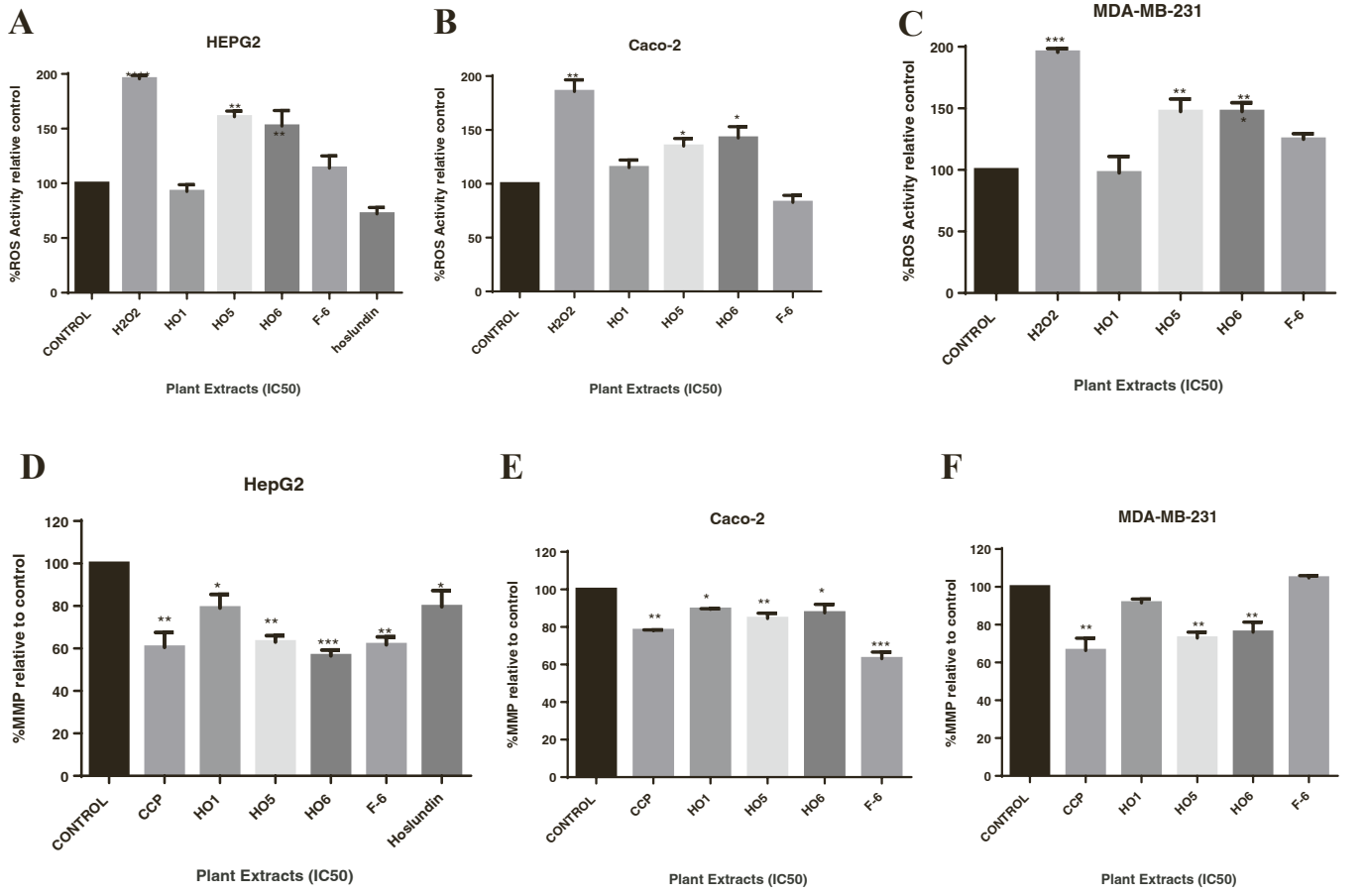

Fig. 7. Inhibition of Reactive Oxygen Species generation (A, B, C) and the effect of fractions of *Hoslundia oppositta* leaves on mitochondria membrane potentials (D, E, F) in HepG2, Caco-2 and MDA-MB-231. NS- Not significant, Values with *, **, *** are significantly different ($P \leq 0.05$) according to ANOVA and Tukey's multiple comparison tests. Each bar A-F represents mean ± SEM, and their level of significance ($P \leq 0.05$) indicated by an asterisk (*) between the control and the treated cells. H2O2- Hydrogen peroxide.

Table 3
NMR data for hoslundin (400 MHz for ^{1}H and 100 MHz for ^{13}C, $CDCl_3$).

Position	δ_C	δ_H (mult., *J*, Hz)	HMBC
4	182.4		
4″	173.3		
2	164		
7	163.9		
9	159.5		
5	158.3		
2″	158.2		
6″	153.7	7.73 (s, 1 H, H-6″)	F-6, C-5", C-2", C-4"
3″	145.1		
4′	131.9	7.55 (m, 3 H, H-4′, 2 H-3′5′)	C-1′, C-2′,6′
1′	131.2		
3′5′	129.1	7.55 (m, 3 H, H-4′, 2 H-3′5′)	
2′6′	126.3	7.91 (dd, *J* = 7.9, 1.7 Hz, 2 H-2′6′)	C-1′, C-3′,5′
5″	121.4		
3	106.1	6.70 (s, 1 H, H-3)	C-10, C-1′, C-2, C-4
10	105.8		
6	103.7		
8	90.3	6.59 (s, 1 H, H-8)	F-6, C-10, C-5, C-7, C-4
8"	60.1	3.91 (s,3 H, OCH_3)	C-3"
11	56.4	3.88 (s, 3 H, OCH_3)	C-7
7"	14.8	2.38 (s, 3 H, CH_3)	C-8", C-3", C-2″
OH	–	13.02 (s, 1 H)	

Table 4
IC_{50} data of the tested fractions of *Hoslundia opposita* leaves.

Plant Extracts	Caco-2 (μg/mL)	MDA-MB-231 (μg/mL)	HepG2 (μg/mL)	HaCaT (μg/mL)
DOX	70	65	38	16
HO1	62	70	23	136
HO5	28	33	15	95
HO6	30	26	11	111
F-6	51	24	17	58
Hoslundin	83	254	27	132

scavenger action of ROS that probably destroy mitochondrial membrane limiting the mitochondrial membrane potential but with subsequent release of cytochrome c. The cytochrome c release induces caspase-3 activities resulting in mitochondria/cytochrome-induced cancer cell death [55], Fig. 3. The integrity of the cell is synonymous with mitochondrial potential due to the regulation of mitochondrial protein that determines ATP production and ROS. Hence, changes or alterations in membrane potential lead to cell cycle arrest and apoptosis due to impaired metabolic activity as shown in Fig. 5A–C. The results depict that **HO1**, **HO5**, **HO6**, **F-6**, and hoslundin are inducers of ROS in cancer cell lines which cause reduced membrane mitochondrial potential via activation of mitochondria/cytochrome c signaling pathway as revealed in increase activity of caspases 3/7, hence regarded as potential anti-cancer agents for clinical.settings (Scheme 1.

In conclusion, this study successfully identified hoslundin from a bio-guided fractionation assay with characteristic selectivity and sensitivity in cancer and normal cell lines and specific to HepG2 cells compared with other cell lines used in this study. The results of this study showed anti-proliferative activity of hoslundin and fractions of *Hoslundia*

opposita leaves via mitochondrial-dependent ROS generation resulting in apoptosis. This work revealed that the treatments could be the most sought-after anticancer therapy that may be adopted as tailor-designed drugs specific for particular cancer types. Thus, the *in vivo* anticancer effect of purified hoslundin and its underlying molecular mechanism is strongly recommended.

Funding

The authors funded the research outcome presented in this article.

CRediT authorship contribution statement

Abosede Christiana Ajibare: Conceptualization, most plant extraction and its experiment, most cell culture experiment, Writing – original draft, Writing – review & editing, Data analysis, Visualization. **Osaretin Albert Taiwo Ebuehi:** Conceptualization, Writing – review & editing, Supervision. **Rahmat Adetutu Adisa:** Conceptualization, Writing – review & editing, Supervision. **Margaret Oluwatoyin Shofidiya:** most plant extraction and its experiment. **Joseph A.O. Olugbuyiro:** most plant extraction and its experiment. **Kolajo Adedamola Akinyede:** most cell culture experiment, Writing – original draft, Visualization. **Helen Adeola Iyiola:** most plant extraction and its experiment. **Yusuf Adeyemi Adegoke:** NMR Data analysis, Writing – original draft, Writing – review & editing. **Sylvester Ifeanyi Omoruyi:** Conceptualization, most cell culture experiment, Writing – review & editing. **Okobi Eko Ekpo:** Conceptualization, Writing – review & editing, Supervision. All authors have read and agree to the publishing of this manuscript. All data were generated in-house; no paper mill was used. We are accountable for all aspects of this research attesting to integrity and accuracy.

Author's declaration

There are no known conflicts of interest associated with this article publication. There has been no significant financial support for this work that could have influenced its outcome.

Conflict of interest statement

All authors, therefore, declare that there is no potential or intending conflict of interest regarding this article.

Appendix A. Supplementary material

Supplementary data associated with this article can be found in the online version at doi:10.1016/j.biopha.2022.113475.

References

[1] H. Sung, J. Ferlay, R.L. Siegel, M. Laversanne, I. Soerjomataram, A. Jemal, F. Bray, Global cancer statistics 2020: GLOBOCAN estimates of incidence and mortality worldwide for 36 cancers in 185 countries, CA Cancer J. Clin. 71 (3) (2021) 209–249.
[2] T. Otto, P. Sicinski, Cell cycle proteins as promising targets in cancer therapy, Nat. Rev. Cancer 17 (2) (2017) 93–115.
[3] T. Rajavel, R. Mohankumar, G. Archunan, K. Ruckmani, K.P. Devi, Beta-sitosterol and daucosterol (phytosterols identified in Grewia tiliaefolia) perturb cell cycle and induce apoptotic cell death in a549 cells, Sci. Rep. 7 (2017) 1–15.
[4] M.S.I. Abaza, K.Y. Orabi, E. Al-Quattan, J. Raja'a, Growth inhibitory and chemosensitization effects of naringenin, a natural flavanone purified from Thymus vulgaris, on human breast and colorectal cancer, Cancer Cell Int. 15 (2015) 46.
[5] V.J. Ram, S. Kumari, Natural products of plant origin as anticancer agents, Drug News Perspect. 14 (2001) 465–482.
[6] E. Solowey, M. Lichtenstein, S. Sallon, H. Paavilainen, E. Solowey, H. Lorberboum-Galski, Evaluating medicinal plants for anticancer activity, Sci. World J., 2014, p. 12.
[7] T. Rajavel, R. Mohankumar, G. Archunan, K. Ruckmani, K.P. Devi, Beta-sitosterol and daucosterol (phytosterols identified in Grewia tiliaefolia) perturb cell cycle and induce apoptotic cell death in a549 cells, Sci. Rep. 7 (2017) 1–15.
[8] K.A. Akinyede, O.E. Ekpo, O.O. Oguntibeju, Ethnopharmacology, therapeutic properties and nutritional potentials of Carpobrotus edulis: a comprehensive review, Sci. Pharm. 88 (2020) 16.
[9] K. Takahashi, S. Kawaguchi, K. Nishimura, K. Kubota, Y. Tanabe, M. Takani, Chem. Pharm. Bull. (1974) 2232–2233.
[10] D.K. Abbiw, Useful Plants of Ghana, IntermediateTechnology Publications LTD. and the Royal Botanic Gardens Kew, London, 1990.
[11] O. Olajide, O. Oladiran, S. Awe, J. Makinde, Pharmacological evaluation of hoslundia opposita extract in rodents, Phytother. Res. Int. J. Devoted Pharmacol. Toxicol. Eval. Nat. Prod. Deriv. 12 (1998) 364–366.
[12] G. Gundidza, S. Deans, K. Svoboda, S. Mavi, Antimicrobial activity of essential oil from hoslundia opposita, Cent. Afr. J. Med. 38 (1992) 290–293.
[13] M.J. Moshi, D.F. Otieno, P.K. Mbabazi, A. Weisheit, The ethnomedicine of the haya people of bugabo ward, Kagera region, northwestern Tanzania, J. Ethnobiol. Ethnomed. 5 (2009) 1–5.
[14] L. Usman, M. Zubair, S. Adebayo, I. Oladosu, N. Muhammad, J. Akolade, Chemical composition of leaf and fruit essential oils of hoslundia opposita Vahl grown in Nigeria, Am.-Eurasian J. Agric. Environ. Sci. 8 (2010) 40–43.
[15] H. Achenbach, R. Waibel, M.H. Nkunya, H. Weenen, Antimalarial compounds from hoslundia opposita, Phytochemistry 31 (1992) 3781–3784.
[16] J.O. Akolade, L.A. Usman, O.E. Okereke, N.O. Muhammad, Antidiabetic potentials of essential oil extracted from the leaves of hoslundia opposita Vahl, J. Med. Food 17 (2014) 1122–1128.
[17] B.T. Ngadjui, A. Tsopmo, J.F. Ayafor, J.D. Connolly, H. Tamboue, Hosloppin, a new pyrone-substituted flavonoid from hoslundia opposita, J. Nat. Prod. 58 (1995) 109–111.
[18] B.T. Ngadjui, J.F. Ayafor, B.L. Sondengam, J.D. Connolly, D.S. Rycroft, Hoslundin, hoslundal, and hoslunddiol: three new flavonoids from the twigs of hoslundia opposita (Lamiaceae), Tetrahedron 47 (1991) 3555–3564.
[19] S.A. Fadeyi, O.O. Fadeyi, A.A. Adejumo, et al., *In vitro* anticancer screening of 24 locally used Nigerian medicinal plants, BMC Complement. Altern. Med. 13 (2013) 79.
[20] O.O. Ogbole, P.A. Segun, A.J. Adeniji, In vitro cytotoxic activity of medicinal plants from Nigeria ethnomedicine on Rhabdomyosarcoma cancer cell line and HPLC analysis of active extracts, BMC Complement. Altern. Med 17 (1) (2017) 494, https://doi.org/10.1186/s12906-017-2005-8. PMID: 29166892; PMCID: PMC5700537.
[21] J.A. Olugbuyiro, J.O. Moody, M.T. Hamann, Phytosterols from Spondias mombin Linn with antimycobacterial activities, Afr. J. Biomed. Res. 16 (2013) 19–24.
[22] W.C. Evans, Trease and evans, Pharmacognosy, ninth ed., Saunders Elsevier, 2002, pp. 553–557.
[23] A.L. Waterhouse, Determination of total phenolics, Curr. Protoc. Food Anal. Chem. 6 (1) (2002). I1-I1.
[24] A. Sofowora, E. Ogunbodede, A. Onayade, The role and place of medicinal plants in the strategies for disease prevention, Afr. J. Tradit. Complement. Altern. Med. 10 (5) (2013) 210–229.
[25] S. Adeniyi, C. Orjiekwe, J. Ehiagbonare, Determination of alkaloids and oxalates in some selected food samples in Nigeria, Afr. J. Biotechnol. 8 (2009) 110–112.
[26] B. Obadoni, P. Ochuko, Phytochemical studies and comparative efficacy of the crude extracts of some hemostatic plants in Edo and Delta states of Nigeria, Glob. J. Pure Appl. Sci. 8 (2002) 203–208.
[27] Q. Shen, B. Zhang, R. Xu, Y. Wang, X. Ding, P. Li, Antioxidant activity in vitro of the selenium-contained protein from these-enriched bifidobacterium animalis 01, Anaerobe 16 (2010) 380–386.
[28] M. Govindappa, N. Bharath, H. Shruthi, T. Sadananda, P. Sharanappa, Antimicrobial, antioxidant and in vitro anti-inflammatory activity and phytochemical screening of Crotalaria pallida aiton, Afr. J. Pharm. Pharmacol. 5 (2011) 2359–2371.
[29] O. Ahmed, S. Libsu, D. Moges, A study of antioxidant activities of guava (Psidium guajava) and mango (Mangifera indica) fruits, Int. J. Int. Sci. Inn. Tech. Sec. B 2 (3) (2013) 1–5.
[30] R.A. Adisa, G.T. Getti, S.C. Richardson, Antioxidant and anti-proliferative activity of fractions from anona senegalensis pers (Annonaceae) stem bark on HeLa cells, FASEB J. 31 (774) (2017) 718–774, 718.
[31] W.C. Chen, S.S. Liou, T.F. Tzeng, S.L. Lee, I.M. Liu, Wound repair and anti-inflammatory potential of Lonicera japonica in excision wound-induced rats, BMC Complement Altern. Med. 12 (2012) 226.
[32] F.N. Muanda, J. Bouayed, A. Djilani, C. Yao, R. Soulimani, A. Dicko, Chemical composition and, cellular evaluation of the antioxidant activity of Desmodium adscendens leaves, Evid. Based Complement. Altern. Med., 2010, p. 10.
[33] T. Mosmann, Rapid colorimetric assay for cellular growth and survival: application to proliferation and cytotoxicity assays, J. Immunol. Methods 65 (1983) 55–63.
[34] B. Dell Bello, M. Toscano, D. Moretti, E. Mac Ilaro, Cisplatin induced apoptosis, inhibits autophagy, which acts as a pro-survival mechanism in human melanoma cells, PLoS ONE 8 (2) (2013), e57236.
[35] F. Karakuş, E. Eyol, K. Yılmaz, S. Ünüvar, Inhibition of cell proliferation, migration and colony formation of LS174T Cells by carbonic anhydrase inhibitor, Afr. Health Sci. 18 (4) (2018) 1303–1310.
[36] S. Omoruyi, O. Ekpo, D. Semenya, A. Jardine, S. Prince, The exploitation of a novel phenothiazine derivative for its anti-cancer activities in malignant glioblastoma, Apoptosis (2020) 1–14.
[37] Y. Shi, M.L. Zhu, Q. Wu, Y. Huang, X.L. Xu, W. Chen, The potential of drug delivery nanosystems for sepsis treatment, J. Inflamm. Res. 14 (2021) 7065–7077.
[38] N. Zamzami, C. Maisse, D. Metivier, G. Kroemer, Measurement of membrane permeability and permeability transition of mitochondria, in: L.A. Pon, E.A. Schon (Eds.), Methods in Cell Biology, Academic Press, San Diego, 2001, pp. 147–158.

[39] P.B. Tchounwou, S. Dasari, F.K. Noubissi, P. Ray, S. Kumar, Advances in our understanding of the molecular mechanisms of action of cisplatin in cancer therapy, J. Exp. Pharmacol. 13 (2021) 303–328.
[40] A. Ghantous, A. Sinjab, Z. Herceg, N. Darwiche, Parthenolide: from plant shoots to cancer roots, Drug Discov. Today 18 (2013) 894–905.
[41] M.S.I. Abaza, K.Y. Orabi, E. Al-Quattan, J. Raja'a, Growth inhibitory and chemosensitization effects of naringenin, a natural flavanone purified from Thymus vulgaris, on human breast and colorectal cancer, Cancer Cell Int. 15 (2015) 46.
[42] S. Ullah Khan, T.A. Saleh, A. Wahab, M.H.U. Khan, D. Khan, W. Ullah Khan, A. Rahim, S. Kamal, F. Ullah Khan, S. Fahad, Nanosilver: new ageless and versatile biomedical therapeutic scaffold, Int. J. Nanomed. 13 (2018) 733–762.
[43] S. Quideau, D. Deffieux, C. Douat-Casassus, L. Pouysegu, Plant polyphenols: chemical properties, biological activities, and synthesis, Angew. Chem. Int. Ed. 50 (2011) 586–621.
[44] J. Dai, R.J. Mumper, Plant phenolics: extraction, analysis, and their antioxidant and anticancer properties, Molecules 15 (2010) 7313–7352.
[45] C. Yang, S.R. Gundala, R. Mukkavilli, S. Vangala, M.D. Reid, R. Aneja, Synergistic interactions among flavonoids and acetogenins in Graviola (Annona muricata) leaves confer protection against prostate cancer, Carcinogenesis 36 (2015) 656–665.
[46] S. Pandey, C. Walpole, P.N. Shaw, P.J. Cabot, A.K. Hewavitharana, J. Batra, Bioguided fractionation of papaya leaf juice for delineating the components responsible for the selective anti-proliferative effects on prostate cancer cells, Front. Pharmacol. 9 (1319) (2018) 10.
[47] N. Chainani-Wu, Safety and anti-inflammatory activity of curcumin: a component of Tumeric (Curcuma longa), J. Altern. Complement. Med. 9 (2003) 161–168.
[48] M. Saikali, A. Ghantous, R. Halawi, S.N. Talhouk, N.A. Saliba, N. Darwiche, Sesquiterpene lactones isolated from indigenous middle eastern plants inhibit tumor promoter-induced transformation of jb6 cells, BMC Complement. Altern. Med. 12 (2012) 1–10.
[49] W.N. Shebaby, M.A. Mroueh, P. Boukamp, R.I. Taleb, K. Bodman-Smith, M. El-Sibai, C.F. Daher, Wild carrot pentane-based fractions suppress proliferation of human HACAT keratinocytes and protect against chemically-induced skin cancer, BMC Complement. Altern. Med. 17 (36) (2017) 14.
[50] J.-D. Hsu, S.-H. Kao, T.-T. Ou, Y.-J. Chen, Y.-J. Li, C.-J. Wang, Gallic acid induces g2/m phase arrest of breast cancer cell mcf-7 through stabilization of p27kip1 attributed to disruption of p27kip1/skp2 complex, J. Agric. Food Chem. 59 (2011) 1996–2003.
[51] A.K. Taraphdar, M. Roy, R. Bhattacharya, Natural products as inducers of apoptosis: implication for cancer therapy and prevention, Curr. Sci. (2001) 1387–1396.
[52] C. Eroğlu, M. Seçme, G. Bağcı, Y. Dodurga, Assessment of the anticancer mechanism of ferulic acid via cell cycle and apoptotic pathways in human prostate cancer cell lines, Tumor Biol. 36 (2015) 9437–9446.
[53] W.S. hin, J. Han, R. Kumar, G.G. Lee, J.L. Sessler, J.-H. Kim, J.S. Kim, Programmed activation of cancer cell apoptosis: a tumor-targeted phototherapeutic topoisomerase inhibitor, Sci. Rep. 6 (2016) 1–11.
[54] D. Trachootham, Y. Zhou, H. Zhang, Y. Demizu, Z. Chen, H. Pelicano, P.J. Chiao, G. Achanta, R.B. Arlinghaus, J. Liu, Selective killing of oncogenically transformed cells through a ROS-mediated mechanism by β-phenylethyl isothiocyanate, Cancer Cell 10 (2006) 241–252.
[55] S. Marchi, C. Giorgi, J.M. Suski, C. Agnoletto, A. Bononi, M. Bonora, E. De Marchi, S. Missiroli, S. Patergnani, F. Poletti, Mitochondria-ros crosstalk in the control of cell death and aging, J. Signal Transduct. (2012) 858–864.